Supplementary Material

of

Experimental and Theoretical Study of Bi_2O_2SE Under Compression

A.L.J. Pereira,[1,2*] D. Santamaría-Pérez,[3] J. Ruiz-Fuertes,[3,4] F.J. Manjón,[1*] V.P. Cuenca-Gotor,[1] R. Vilaplana,[5] O. Gomis,[5] C. Popescu,[6] A. Muñoz,[7] P. Rodríguez-Hernández,[7] A. Segura,[3] L. Gracia,[8] A. Beltrán,[9] P. Ruleova,[10] C. Drasar[10] and J. A. Sans[1]

[1] *Instituto de Diseño para la Fabricación y Producción Automatizada, MALTA Consolider Team, Universitat Politècnica de València, València, Spain*

[2] *Grupo de Pesquisa de Materiais Fotonicos e Energia Renovável - MaFER, Universidade Federal da Grande Dourados, Dourados, MS, Brazil*

[3] *Departament de Física Aplicada – ICMUV, MALTA Consolider Team, Universitat de València, Burjassot, Spain*

[4] *DCITIMAC, MALTA Consolider Team, Universidad de Cantabria, Santander, Spain*

[5] *Centro de Tecnologías Físicas, MALTA Consolider Team, Universitat Politècnica de València, València, Spain*

[6] *CELLS-ALBA Synchrotron Light Facility, 08290 Cerdanyola, Barcelona, Spain*

[7] *Departamento de Física, Instituto de Materiales y Nanotecnología, MALTA Consolider Team, Universidad de La Laguna, Tenerife, Spain*

[8] *Departament de Química Física, MALTA Consolider Team, Universitat de València, Burjassot, Spain*

[9] *Departament de Química Física i Analítica, MALTA Consolider Team, Universitat Jaume I, Castellón, Spain*

[10] *Faculty of Chemical Technology, University of Pardubice, Pardubice, Czech Republic*

* Corresponding authors, Email: andrepereira@ufgd.edu.br, fjmanjon@fis.upv.es

Structural data of Bi_2O_2Se under pressure

Table S1. Lattice parameters and unit cell volumes of Bi_2O_2Se obtained from synchrotron XRD experiments at different pressures.

P(GPa)	a axis (Å)	c axis (Å)	V (Å^3)
0.49(3)	3.8823(8)	12.184(3)	183.65(9)
0.68(3)	3.8792(7)	12.167(3)	183.10(8)
1.23(3)	3.8718(6)	12.126(2)	181.79(7)
1.47(3)	3.8683(6)	12.106(2)	181.16(7)
1.97(4)	3.8620(5)	12.072(2)	180.05(5)
2.59(3)	3.8543(6)	12.032(3)	178.75(7)
3.00(4)	3.8498(4)	12.004(2)	177.91(4)
3.57(5)	3.8422(6)	11.967(2)	176.66(6)
5.38(6)	3.8231(7)	11.871(3)	173.50(8)
6.01(5)	3.8159(5)	11.832(2)	172.29(7)
6.99(6)	3.8062(5)	11.785(2)	170.73(5)
7.99(7)	3.7982(17)	11.738(6)	169.34(17)
8.5(1)	3.793(2)	11.710(8)	168.5(2)
9.6(2)	3.788(3)	11.675(12)	167.5(3)
11.9(2)	3.7786(18)	11.629(7)	166.03(19)
12.4(2)	3.7754(19)	11.611(8)	165.5(2)
13.2(2)	3.7724(15)	11.591(9)	164.95(19)
14.5(3)	3.770(3)	11.567(12)	164.4(3)
15.2(2)	3.767(3)	11.549(13)	163.9(3)
15.8(3)	3.763(3)	11.526(13)	163.2(3)
16.3(3)	3.761(3)	11.507(13)	162.8(3)
18.2(4)	3.753(4)	11.465(15)	161.4(4)
19.9(4)	3.744(3)	11.422(16)	160.1(4)
21.7(4)	3.735(4)	11.382(19)	158.8(4)

Vibrational modes in Bi_2O_2Se at the Γ point

Bi_2O_2Se crystallizes in the tetragonal body-centered *I4/mmm* structure and has two formula units in the primitive cell, therefore, it has 10 normal vibrational modes at Γ whose mechanical decomposition is[1]:

$$\Gamma = 1\ A_{1g}(R) + 2\ A_{2u}(IR) + 1\ B_{1g}(R) + 2\ E_u(IR) + 2\ E_g(R) + A_{2u} + E_u$$

where A_{1g}, B_{1g} and E_g modes are Raman-active (R) and A_{2u} and E_u are infrared-active (IR). In total, there are four Raman-active modes ($\Gamma_{Raman} = A_{1g} + B_{1g} + 2E_g$), four infrared-active (IR) modes ($\Gamma_{IR} = 2A_{2u} + 2E_u$) and two acoustic modes ($\Gamma_{Acoustic} = A_{2u} + E_u$). It must be mentioned that that E modes are doubly degenerated. The assignment of the vibrational modes to atomic movements can be done thanks to the program J-ICE[2] that reads OUTCAR files of VASP.

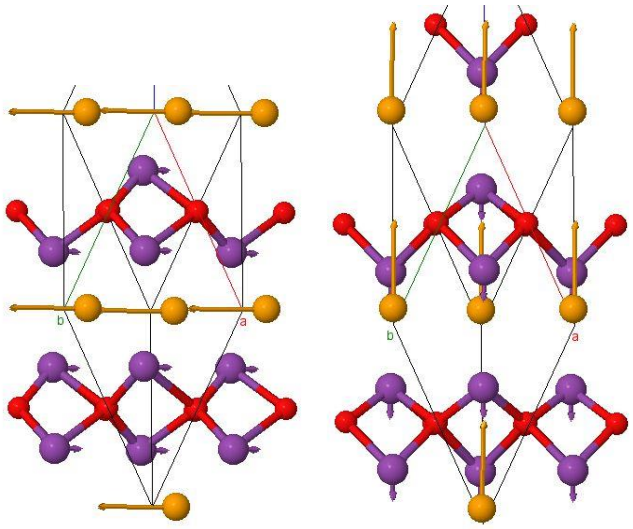

Figure S1. Atomic movements of low-frequency interlayer vibrational modes E_u and A_{2u}.

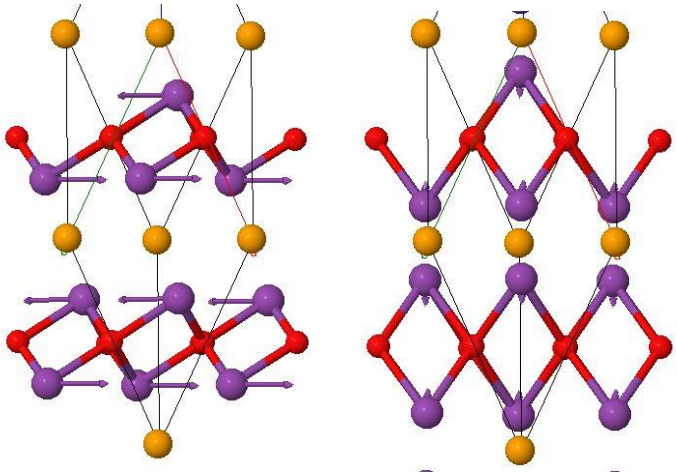

Figure S2. Atomic movements of low-frequency interlayer E_g and A_{1g} vibrational modes.

It is well-known that in layered materials, which usually crystallize either in a hexagonal or tetragonal space group, the lowest-frequency E (doubly degenerated) and A (or B) modes at the Γ point can be classified as interlayer (out-of-phase vibrations of atoms corresponding to adjacent layers) or intralayer (out-of-phase vibrations of atoms inside the layers) modes. Interlayer E and A (or B) modes are usually related to shear or transversal vibrations between adjacent layers along the layer plane (*a*-*b*) and to longitudinal vibrations of one layer against the adjacent ones (along the *c* axis), respectively. Both E and A (or B) interlayer modes come from transversal acoustic (TA) and longitudinal acoustic (LA) modes, respectively, due to the folding of points of the Brillouin zone border into the Γ point due to the decreasing symmetry from cubic to hexagonal or tetragonal. Similarly, E and A (or B) intralayer modes come from transversal optic (TO) and longitudinal optic (LO) modes at Γ and from additional modes due to the folding of the BZ border into the Γ point.

The number of interlayer and intralayer modes in layered materials depends on the complexity of the unit cell. In the simplest case, there should be two interlayer modes and four intralayer modes. In the case of Bi_2O_2Se, there are four interlayer modes (E_u, A_{2u}, E_g and A_{1g}) having the lowest frequencies, while the four intralayer modes (E_u, B_g, A_{2u} and E_g) have the highest frequencies. The two modes with lowest frequency, E_u and A_{2u}, are IR-active and correspond to out-of-phase movements of Se and Bi atoms (see **Fig. S1**); i.e. both modes are typical interlayer modes of layered structures. In fact, they correspond to the shear mode between Bi_2O_2 and Se layers in the layer plane and to

the longitudinal vibration of the Bi_2O_2 and Se layers one against the other along the *c* axis (perpendicular to the layer plane). On the other hand, the low-frequency E_g and A_{1g} modes are Raman-active and correspond to out-of-phase Bi movements in the layer plane and perpendicular to the layer plane, respectively (see **Fig. S2**). These two modes are not so typical of layered materials and come from the fact that there are two Bi_2O_2 layers in the unit cell so that these two modes can be considered as the complementary movements of Bi atoms in the two low-frequency E_u and A_{2u} modes. In these two modes, there is an in-phase movement of Bi atoms in a Bi_2O_2 layer, while in the two low-frequency E_g and A_{1g} modes there is an out-of-phase movement of Bi atoms in the layer. Therefore, the two low-frequency E_u and A_{2u} modes are proper interlayer modes between Bi_2O_2 and Se layers, while the two low-frequency E_g and A_{1g} modes are half interlayer modes between Bi_2O_2 and Se layers and half interlayer modes between the upper and lower halves of each Bi_2O_2 layer.

In layered compounds with typical van der Waals gap between the layers, the low-frequency interlayer shear mode exhibits a much smaller pressure coefficient than other modes, whereas the low-frequency A (or B) mode displays the largest pressure coefficient. For example, the E and A modes with frequencies around 40 (60) cm^{-1} and 116 (133) cm^{-1} in InSe (GaSe) have pressure coefficients of 0.68 (0.85) cm^{-1}/GPa and 5.41 (5.78) cm^{-1}/GPa, respectively[3,4]. Usually, the small pressure coefficient of the low-frequency E mode in layered materials is ascribed to the weak bending force constant due to weak van der Waals forces between the neighboring layers. On the other hand, the large pressure coefficient of the low-frequency A mode is due to the extraordinary increase of the stretching force constant between neighboring layers due to the strong decrease of the interlayer distance[3,4]. A similar behavior is found in layered topological insulators Bi_2Se_3, Bi_2Te_3 and Sb_2Te_3[5-7]. However, a different behavior was recently observed in layered BiTeBr and BiTeI, which also feature a van der Waals gap between the layers[8]. In these semiconductors, the low-frequency E_1(TO) mode has a similar pressure coefficient (4.3 and 3.5 cm^{-1}/GPa, respectively) than the rest of the optic modes and the low-frequency A_1(TO) mode has not so large pressure coefficient (4.5 and 4.6 cm^{-1}/GPa, respectively) as expected for a van der Waals compound. This result suggests that interlayer forces in these two compounds are stronger than common van der Waals forces in other layered compounds, likely due to the asymmetry of the layers what causes a strong polarity of bismuth tellurohalides[9]. Moreover, the rather similar pressure

coefficients of these two modes in BiTeBr and BiTeI also suggests that bending and stretching interlayer bonds tend to harden at similar rates with pressure in both compounds; i.e., the anisotropy in the properties along the layers and perpendicular to the layers is not so high as in other layered compounds and tend to disappear at a similar rate with increasing pressure in both compounds.

The case of Bi_2O_2Se is similar to that of BiTeBr and BiTeI because both interlayer E_u and A_{2u} modes show pressure coefficients of 5.5 and 4.1 cm^{-1}/GPa, respectively. **Figure S3** shows the pressure dependence of the theoretical IR-active modes of Bi_2O_2Se. Therefore, the same explanation already given for the interlayer modes in BiTeBr and BiTeI seems to be valid for Bi_2O_2Se; i.e. interlayer bonding forces are of the same order or stronger that in polar van der Waals compounds, like BiTeBr and BiTeI, and clearly much larger than in non-polar van der Waals compounds, like GaSe and InSe. Curiously, the two interlayer E_g and A_{1g} modes in Bi_2O_2Se have pressure coefficients of 1.1 and 2.1 cm^{-1}/GPa. In this case, the shear mode has a small pressure coefficient as in van der Waals compounds, but the longitudinal mode has a very small pressure coefficient as compared to van der Waals compounds. In summary, we can say that both shear interlayer modes (E_u and E_g) and longitudinal interlayer modes (A_{2u} and A_{1g}) have an average pressure coefficient around 3.2 cm^{-1}/GPa in Bi_2O_2Se, thus suggesting that this is a 2D material with bonding interlayer forces between Bi_2O_2 and Se layers considerably stronger than common van der Waals layered compounds.

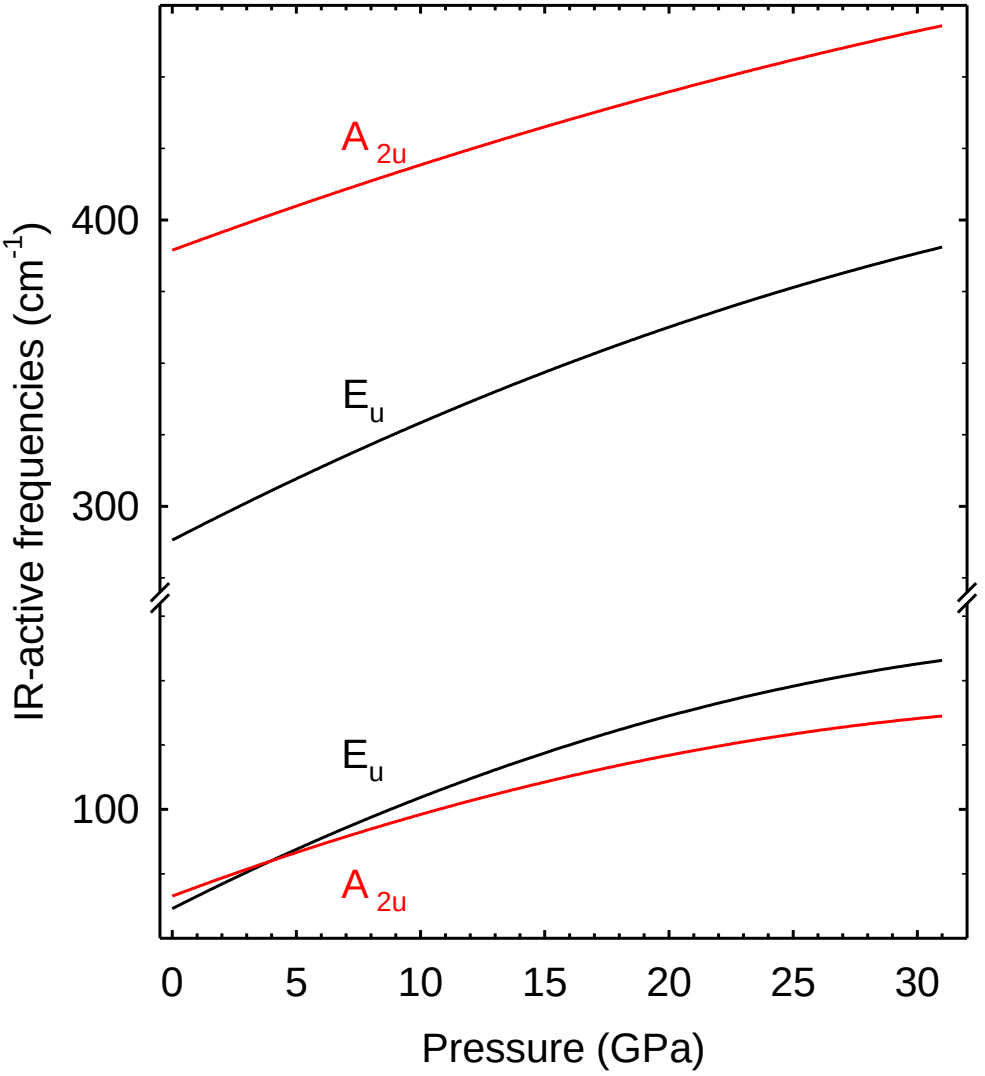

Figure S3. Theoretical pressure dependence of the IR-active modes of Bi_2O_2Se. Different colors represent IR-active modes of different symmetries.

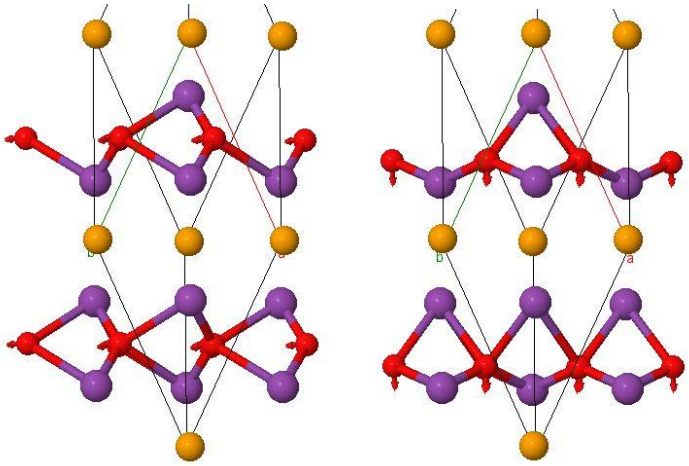

Figure S4. Atomic movements of high-frequency intralayer E_u and A_{2u} vibrational modes.

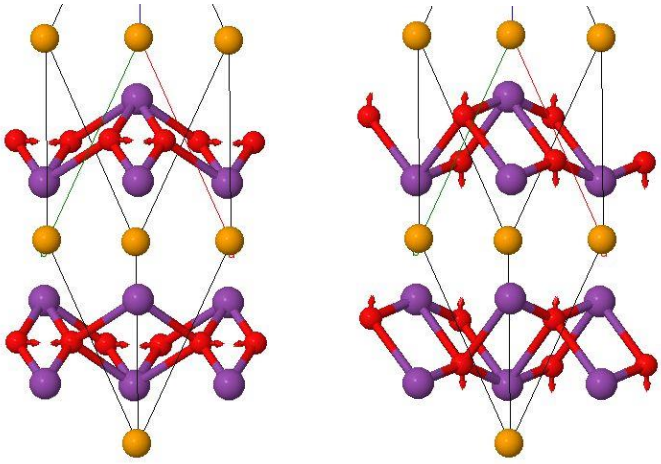

Figure S5. Atomic movements of high-frequency intralayer E_g and B_g vibrational modes.

As regards the high-frequency modes in Bi_2O_2Se, they are intralayer modes related to atomic vibrations of O atoms inside the Bi_2O_2 layers. The two high-frequency E_u and A_{2u} modes are IR-active and correspond to in-phase movements of O atoms in the layer plane and perpendicular to the layer plane, respectively (see **Fig. S4**) and E_g and B_g modes are Raman-active and correspond to out-of-phase movements of O atoms inside the Bi_2O_2 layer in the layer plane and perpendicular to the layer plane, respectively (see **Fig. S5**). As regards the pressure coefficients of all these intralayer modes, they are between 3.0 and 5.3 cm^{-1}/GPa which are typical of bending and stretching modes of ionic-covalent bonds as the Bi-O bonds in Bi_2O_3[10,11]. In fact, the average pressure coefficient of the transversal and longitudinal modes is 3.7 and 2.9 cm^{-}

^{1}/GPa, which are values that are in good agreement with the largest value of transversal than longitudinal modes in most ionic-covalent semiconductors[12].

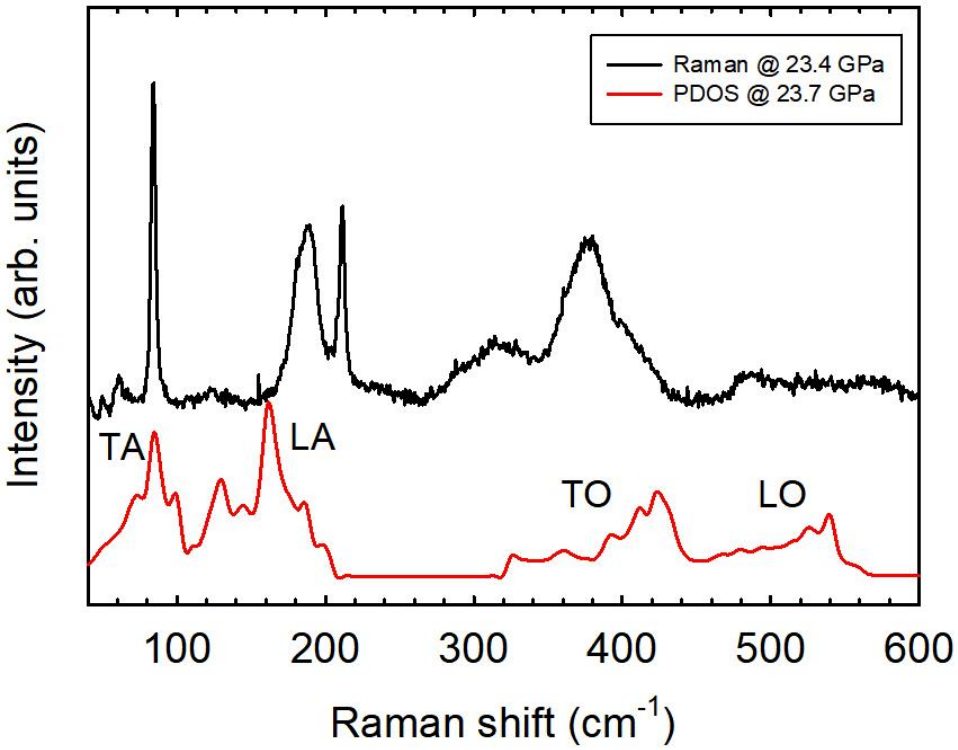

Figure S6. Comparison of the Raman spectrum of Bi_2O_2Se at 23.4 GPa and the theoretical one-phonon density of states at 23.7 GPa.

The RS spectrum of Bi_2O_2Se at 23 GPa shows the two narrow first-order Raman peaks E_g and A_{1g} near 85 and 215 cm^{-1}, respectively. The comparison of RS spectra at 23 GPa with the one-phonon density of states (PDOS) suggests that the other broad bands could originate from one-phonon density of states due to defect assisted Raman scattering. In particular, the broad band at 180-190 cm^{-1} could be assigned to the scattering from the top phonon band of the acoustic region (below 210 cm^{-1}) that corresponds to the longitudinal acoustic (LA) region in binary semiconductors. On the other hand, the broad band between 260 and 450 cm^{-1} could be likely assigned to the scattering of the optic transveral (TO) region and other weaker bands at higher frequencies could be likely due to the scattering of the optic longitudinal (LO) region. No clear sign of the PDOS related to the TA region seems to be observed in the RS spectrum.

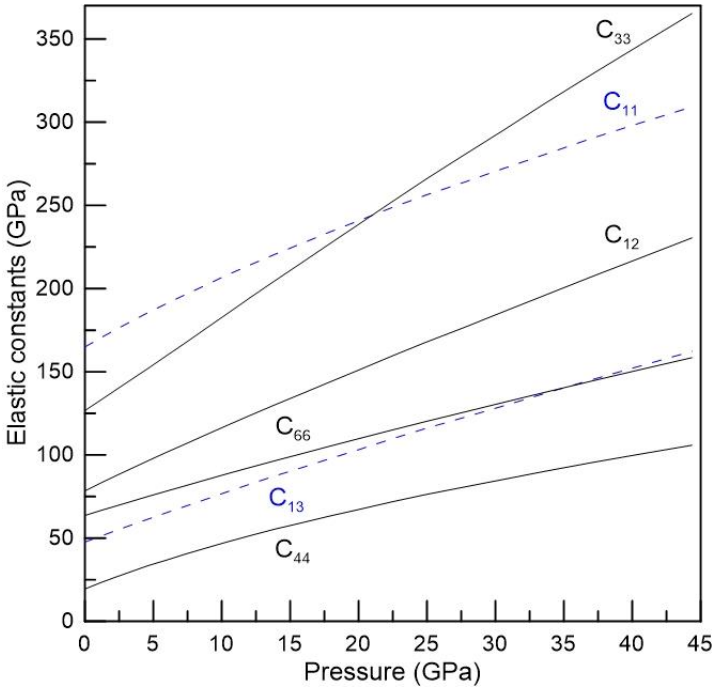

Figure S7. Pressure dependence of theoretical elastic constants, C_{ij}, calculated with VASP in Bi_2O_2Se.

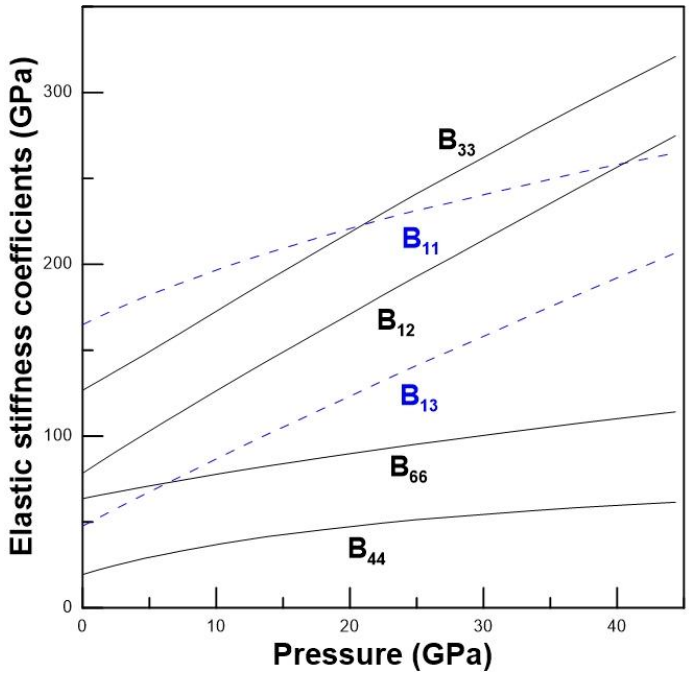

Figure S8. Pressure dependence of theoretical elastic stiffness coefficients, B_{ij}, calculated with VASP in Bi_2O_2Se.

The generalized stability criteria for a body-centered tetragonal lattice[13,14] are given by:

$$M_1 = C_{11} - P > 0$$

$$M_2 = C_{11} - C_{12} - 2P > 0$$

$$M_3 = (C_{33} - P)(C_{11} + C_{12}) - 2(C_{13} + P)^2 > 0$$

$$M_4 = C_{44} - P > 0$$

$$M_5 = C_{66} - P > 0$$

Density of States of Bi_2O_2Se

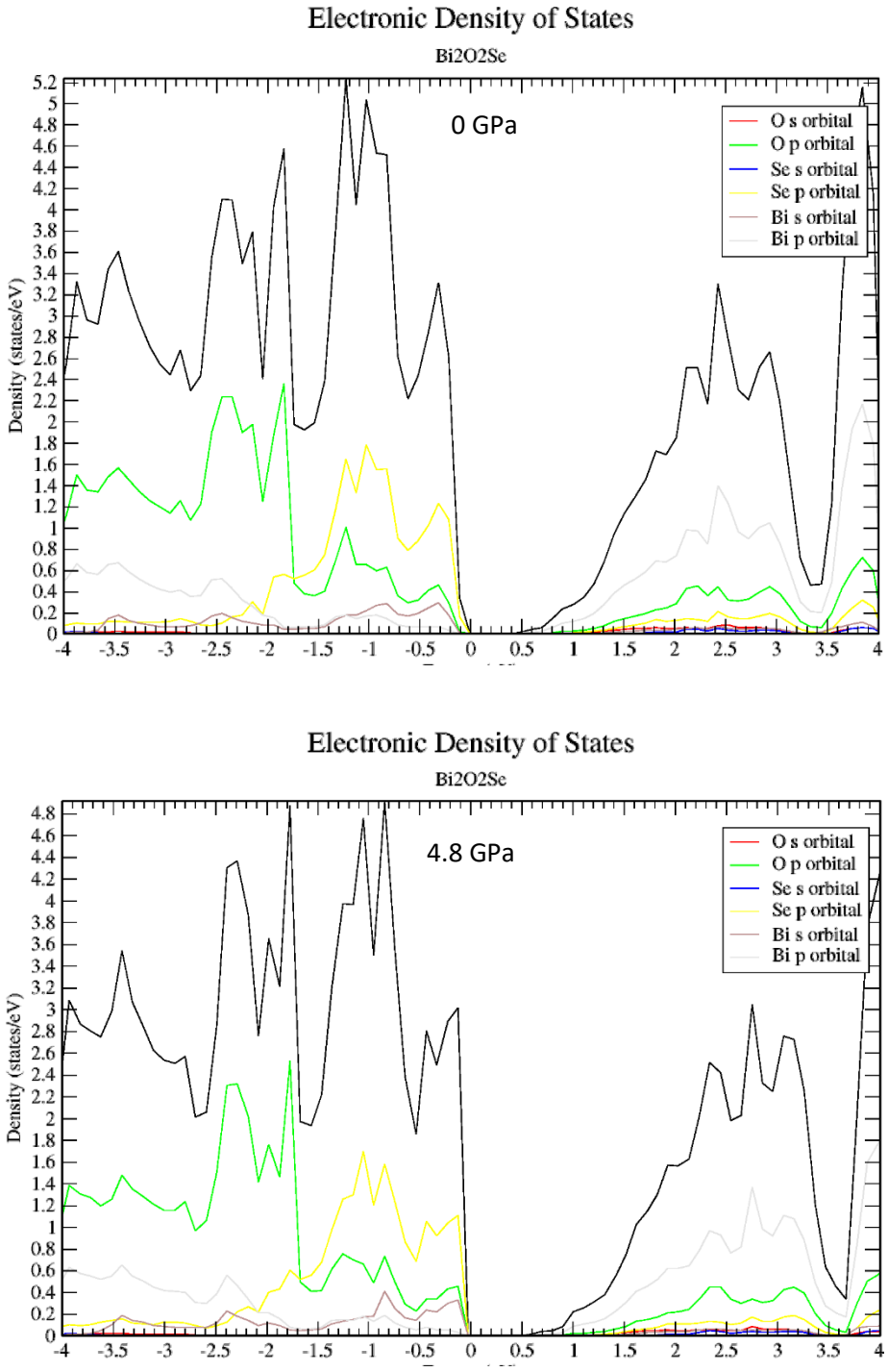

Figure S9. Electronic density of states (DOS) at 0 and 4.8 GPa showing the change of the bandgap with pressure in Bi_2O_2Se.

References

1. Kroumova, E.; Aroyo, M. I.; Perez Mato, J. M.; Kirov, A.; Capillas, C.; Ivantchev, S.; Wondratschek, H. Bilbao Crystallographic Server: Useful Databases and Tools for Phase Transitions Studies. *Phase Trans.* **2003**, *76*, 155-170.
2. Canepa, P.; Hanson, R. M.; Ugliengo, P.; Alfredsson, M. J-ICE: A New Jmol Interface for Handling and Visualizing Crystallographic and Electronic Properties. *J. Appl. Cryst.* **2011**, *44*, 225-229.
3. Ulrich, C.; Mroginski, M. A.; Goñi, A. R.; Cantarero, A.; Schwarz, U.; Muñoz, V.; Syassen, K. Vibrational Properties of InSe under Pressure: Experiment and Theory. *Phys. Stat. Sol. (b)* **1996**, *198*, 121-127.
4. Kulibekov, A. M.; Olijnyk, H. P.; Jephcoat, A. P.; Salaeva, Z. Y.; Onari, S.; Allakverdiev, K. R. Raman Scattering under Pressure and the Phase Transition in ε-GaSe. *Phys. Stat. Sol (b)* **2003**, *235*, 517-520.
5. Vilaplana, R.; Gomis, O.; Manjón, F. J.; Segura, A.; Pérez-González, E.; RodríguezHernández, P.; Muñoz, A.; González, J.; Marín-Borrás, V.; Muñoz-Sanjosé, V.; et al. High-Pressure Vibrational and Optical Study of Bi_2Te_3. *Phys. Rev. B* **2011**, *84*, 104112.
6. Gomis, O.; Vilaplana, R.; Manjón, F. J.; Rodríguez-Hernández, P.; Pérez-González, E.; Muñoz, A.; Kucek, V.; Drasar, C. Lattice Dynamics of Sb_2Te_3 at High Pressures. *Phys. Rev. B* **2011**, *84*, 174305.
7. Vilaplana, R.; Santamaría-Pérez, D.; Gomis, O.; Manjón, F. J.; González, J.; Segura, A.; Muñoz, A.; Rodríguez-Hernández, E.; Pérez-González, E.; Marín-Borrás, V.; et al. Structural and Vibrational Study of Bi_2Se_3 under High Pressure. *Physical Review B* **2011**, *84*, 184110.

8. Sans, J. A.; Manjón, F. J.; Pereira, A. L. J.; Vilaplana, R.; Gomis, O.; Segura, A.; Muñoz, A.; Rodríguez-Hernández, P.; Popescu, C.; Drasar, C.; et al. Structural, Vibrational, and Electrical Study of Compressed BiTeBr. *Phys. Rev. B* **2016**, *93*, 024110.
9. Ma, Y. D.; Dai, Y.; Wei, W.; Li, X. R.; Huang, B. B. Emergence of Electric Polarity in BiTeX (X = Br and I) Monolayers and the Giant Rashba Spin Splitting. *Phys. Chem. Chem. Phys.* **2014**, *16*, 17603-17609.
10. Pereira, A. L. J.; Gomis, O.; Sans, J. A.; Pellicer-Porres, J.; Manjón, F. J.; Beltran, A.; Rodríguez-Hernandez, P.; Muñoz, A. Pressure Effects on the Vibrational Properties of α-Bi_2O_3: An Experimental and Theoretical Study. *J. Phys.: Cond. Mat.* **2014**, *26*, 225401.
11. Pereira, A. L. J.; Sans, J. A.; Vilaplana, R.; Gomis, O.; Manjón, F. J.; Rodríguez-Hernández, P.; Muñoz, A.; Popescu, C.; Beltrán, A. Isostructural Second-Order Phase Transition of β-Bi_2O_3 at High Pressures: An Experimental and Theoretical Study. *J. Phys. Chem. C* **2014**, *118*, 23189-23201.
12. Manjón, F. J.; Syassen, K.; Lauck, R. Effect of Pressure on Phonon Modes in Wurtzite Zinc Oxide. *High Pressure Research* **2002**, *22*, 299-304.
13. Wallace, D. C. Thermoelasticity of Stressed Materials and Comparison of Various Elastic Constants. *Phys. Rev.* **1967**, *162*, 776-789.
14. Grimvall, G.; Magyari-Köpe, B.; Ozolinš, V.; Persson, K. A. Lattice Instabilities in Metallic Elements. *Rev. Mod. Phys.* **2012**, *84*, 945-986.